SCIENCE CHINA
Technological Sciences

•Article•

February 2019 Vol.62 No.2: 349–355
https://doi.org/10.1007/s11431-018-9370-y

Experimental study on spray cooling under reduced pressures

PENG Can[1], XU XiangHua[1*], LI YeMing[1], LI YuLong[2] & LIANG XinGang[1]

[1] *Key Laboratory for Thermal Science and Power Engineering of Ministry of Education, School of Aerospace Engineering, Tsinghua University, Beijing 100084, China;*
[2] *School of Energy and Power Engineering, Beihang University, Beijing 100191, China*

Received August 25, 2018; accepted October 12, 2018; published online January 4, 2019

Spay cooling is a complicated flow and heat transfer process affected by multi-factors among which the environmental pressure is extremely important. However the influence of pressure is not investigated sufficiently, especially the reduced pressure. In the present study, spray cooling under low initial environmental partial pressures and vapor partial pressures with R21 are investigated with a closed spray and condensation system. To study the influence of initial environmental partial pressure, different amounts of nitrogen are inflated into the vacuum flash chamber, while the vapor partial pressure is kept constant. To study the influence of vapor partial pressure, a cascade refrigerator is used to condense the vapor with different condensation temperatures so that the vapor partial pressure can be maintained or adjusted, while the initial environmental partial pressure is kept constant. The experimental results show that the spray cooling power increases monotonically with the increasing spray flow rate in the experimental range, while the cooling efficiency decreases with the increasing spray flow rate. The spray cooling power and cooling efficiency vary with the initial environmental partial pressure or the vapor partial pressure non-monotonously, which indicates there is an optimal pressure for the heat transfer performance. Besides, the mechanism of the non-monotonous variation trend is discussed based on the key aspects including flash evaporation, convection and boiling. Especially, the boiling heat transfer curve is applied to explain the trend.

spray cooling, flash evaporation, reduced pressure, phase change

Citation: Peng C, Xu X H, Li Y M, et al. Experimental study on spray cooling under reduced pressures. Sci China Tech Sci, 2019, 62: 349–355, https://doi.org/10.1007/s11431-018-9370-y

1 Introduction

Flash spray cooling is a combination of flash evaporation and spray cooling. For the flashing the environmental pressure needs to be much lower than the saturated pressure. Under such condition, the coolant evaporates rapidly and removes a large amount of heat. The high heat dissipation capacity makes the flash spray cooling a very promising candidate for the thermal control of electronic devices.

Spray cooling under normal environmental pressure has been widely investigated. The research interests included the influences of spray mass flux, spray distance, spray inclination, surface structure, droplet diameter, droplet velocity, etc. [1–11]. Cader et al. [12] tried to apply the spray cooling to the chip cooling. They achieved a temperature decrease of 33.3°C and a power consumption reduction of 35% with spray cooling compared with air cooling. Bostanci et al. [13] developed a spray cooling system for power inverter modules. According to the test results, the device temperature could be kept below 125°C with a heat flux up to 330 W/cm^2. Another application of the spray cooling to thermal control for the electronic devices was the CRAY X-1 computer [14].

Investigations concerning the influence of environmental pressure were reported by several researchers. Zhou et al. [2] investigated the transient spray cooling performance under

*Corresponding author (email: xxh@tsinghua.edu.cn)

different environmental pressures. R134a was sprayed onto an epoxy resin substrate and the spray duration was 50 ms. The heat flux first increased to a peak and then dropped to zero. The results revealed that at short spray distances (10 mm) the maximum heat flux increased monotonically with the decreasing pressure, while there was a transitional pressure around 10 kPa for the maximum heat flux at long spray distances. Han [15] experimentally studied the spray cooling capacity and temperature uniformity under different environmental pressures with water. The results showed that low environmental pressures could yield better heat transfer performance than high environmental pressures. When the environmental pressure ranged from 2.5 kPa to 100 kPa the heat flux decreased exponentially. And low environmental pressures improved the temperature uniformity on the heater surface.

Jiang and Dhir [16] investigated the effect of total system pressure and vapor partial pressure with water. Experiments were arranged by keeping the air partial pressure at 3.12 kPa, while increasing the total system pressure from 10.4 kPa to 101 kPa. Other cases by keeping the total system pressure at 101 kPa, while changing the vapor partial pressure from 7.3 kPa to 97.9 kPa were also conducted. The results indicated that non-condensable gas deteriorated the heat transfer performance in the single phase regime, while in the two phase regime the non-condensable gas did not affect the heat transfer performance, but the heat flux would still vary with the total system pressure. The non-condensable gas effect on the spray cooling performance was also studied by Lin and Ponnappan [17] with FC-72 in a closed loop whose results revealed that non-condensable gas increased the total system pressure and shifted the spray cooling curve to the right. Horacek et al. [18] obtained similar results and found that critical heat flux increased with the increasing gas content. Mudawar et al. [19] discussed the viability and implementation to apply the spray cooling to hybrid vehicle electronics. Heat transfer performance under environmental pressure higher than 1 atm was examined. The conclusion was that HFE-7100 instead of R134a could maintain the device temperature below the maximum allowable temperature of 125°C with a heat flux of 200 W/cm^2.

NASA used to develop a cylindrical flash evaporator [20]. The maximum heat dissipation power could reach 38.4 kW. Later, a compact flash evaporation system with an evaporator and two nozzle plates assembled from both sides was also investigated [21]. The evaporator is 150 mm length, 150 mm width and 15 mm height.

From the literature review, most studies focused on the heat transfer performance under normal environmental pressures. Although several of them concerned the effect of different environmental pressures, the heat transfer behavior under low environmental pressure needs further investigation. In the present study, a flash spray cooling experimental system is established. Nitrogen is adopted to create different initial environmental partial pressures and a cascade refrigerator is used to condense the vapor of Freon 21 (R21) with different condensation temperatures so that the vapor partial pressure can be maintained or adjusted. The influences of spray mass flow rate and low pressures on the flash spray cooling performance with R21 are investigated. A non-monotonous variation trend of spray cooling power and cooling efficiency is evidenced, which indicates that there is an optimal pressure for the heat transfer performance. Thus, reducing the initial environmental partial pressure or the vapor partial pressure cannot always benefit the heat transfer. The mechanism of the optimal heat transfer performance will be discussed in three key aspects including flash evaporation, convection and boiling. Especially, the boiling heat transfer curve is applied to explain the trend.

2 Experiment setup

The flash spray cooling system is composed of several subsystems including a spray system, an evaporator system, a refrigerator system, a coolant recovery system, a measurement and data acquisition system, as shown in Figure 1. The spray system is constructed to deliver the spray coolant, R21. With the aid of a gear pump the coolant is pumped out from the reservoir. An ice bucket is setup to subcool the coolant to prevent vaporization in the pump. Downstream from the pump are a valve and a filter followed by a mass flowmeter. An electric heater and a temperature controller are arranged to maintain the temperature of R21 at the inlet of the nozzles which is measured by a sheathed T-type thermocouple. Four Danfoss OD nozzles (1.0GPH60) are assembled above the evaporator in the flash evaporation chamber. The nozzle is a full cone type with a spray angle of 60º. The evaporator system simulates a simple fluid loop that uses the evaporator as a heat sink. The evaporator and nozzle assembly is shown in Figure 2. Water is circulated in the fluid loop driven by a vane pump and the circulation flow rate is measured by another mass flowmeter. The temperature at the inlet of the evaporator is controlled by a thermostatic water tank.

The refrigerator system is used to maintain or adjust the vapor partial pressure. At the beginning of experiments the air in the flash evaporating chamber and condensing chamber will be evacuated by a vacuum pump. Then a given amount of nitrogen will be inflated into the chambers to create an initial environmental partial pressure. After the flash evaporation starts, the vapor will be condensed by the cryogenic refrigerant in the condensing heat exchanger which is supplied by the cascade refrigerator so that the vapor partial pressure can be controlled. The refrigerant could be cooled to –60°C with a refrigeration power of

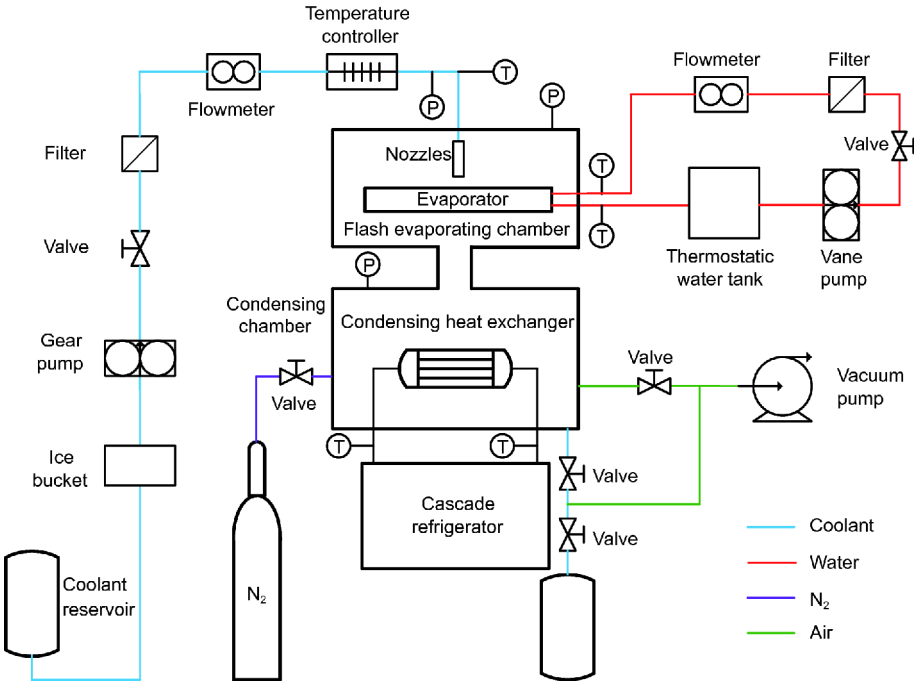

Figure 1 (Color online) Schematic of flash spray cooling system.

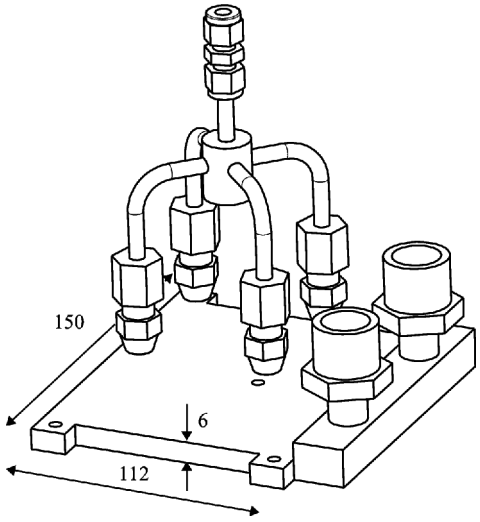

Figure 2 Evaporator and nozzle assembly (dimension: mm).

3.0 kW. Pressures of the flash evaporating chamber and the condensing chamber are measured by two pressure transmitters. At the end of experiments, the R21 will be collected by the coolant recovery system for recycling. The temperature and pressure signals are acquired using National Instruments CompactDAQ NI 9214 and NI 9219.

The flash spray cooling power can be calculated by the enthalpy drop of the water flowing through the evaporator:

$$Q = m_{\mathrm{w}} c_{\mathrm{p}} (T_{\mathrm{in}} - T_{\mathrm{out}}), \tag{1}$$

where m_{w} and c_{p} denotes the water mass flow rate and specific heat capacity respectively, and T_{in} and T_{out} are the inlet and outlet temperatures of the evaporator.

The cooling efficiency is defined as

$$\varepsilon = \frac{Q}{m_{\mathrm{f}}(h_{\mathrm{out}} - h_{\mathrm{in}})}, \tag{2}$$

where h_{in} and h_{out} denotes the enthalpy of R21 at the inlet of nozzles and the saturated vapor enthalpy under the pressure in the flash evaporating chamber respectively, and m_{f} is the spray flow rate of R21.

The measurement uncertainties of pressure, water mass flow rate and R21 mass flow rate are all 0.2%, and the uncertainty of temperature is estimated to be within ± 0.2°C. According to error propagation formula, the relative uncertainties of spray cooling power and cooling efficiency are in the range from 3.5% to 5.8%.

3 Results and discussion

3.1 Effect of spray flow rate

Figure 3 shows the variation of spray cooling power with the spray flow rate for the initial environmental partial pressure at 1.3 kPa. The temperature of R21 at the inlet of the nozzles is 20.0°C and the temperature of water at the inlet of the evaporator is 26.4°C. As shown in Figure 3, when the spray flow rate ranges from 2.04 g/s to 3.93 g/s, the spray cooling power increases monotonically from 397.5 W to 618.7 W.

Figure 4 shows the variation of cooling efficiency with the spray flow rate. In contrast to the spray cooling power, the

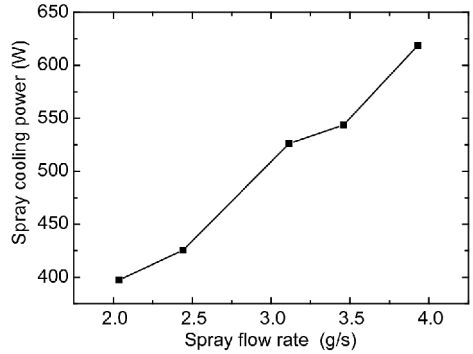

Figure 3 Variation of the spray cooling power with the spray flow rate.

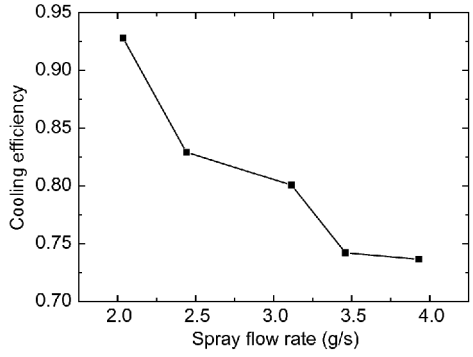

Figure 4 Variation of the cooling efficiency with the spray flow rate.

cooling efficiency shows a decreasing trend with the spray flow rate. At the spray flow rate of 2.04 g/s the cooling efficiency is up to 92.8%, while it drops to 73.6% at the spray flow rate of 3.93 g/s. The reason is that larger spray flow rate causes more droplets to bounce and splash due to higher velocity. Furthermore, larger spray flow rate produces finer droplets [22] which are easier to be carried away by the gas flow and may evaporate out before reaching the evaporator surface because of rapid flash evaporation.

3.2 Effect of reduced pressures

To investigate the effect of initial environmental partial pressure (P_{N2}) on the spray cooling performance, the vapor partial pressure (P_{R21}) calculated by the difference between the total pressure and the initial environmental partial pressure is maintained at 28.0 kPa, while the initial environmental partial pressure changes from 1.8 kPa to 43.6 kPa by injecting different amounts of nitrogen. The spray flow rate is 3.93 g/s. The temperature of R21 at the inlet of the nozzles is set at 17.7°C and the temperature of water at the inlet of the evaporator is set at 19.0°C. Figure 5 shows the variation of spray cooling power with the initial environmental partial pressure. It is noticed that the spray cooling power first increases from 535.7 W to 587.6 W, then decreases to 404.2 W sharply with the initial environmental partial pressure increasing from 1.8 kPa to 43.6 kPa. The cooling efficiency shows a similar variation trend to the spray cooling power as shown in Figure 6. The highest cooling efficiency obtained in Figure 6 is 68.4%, and the cooling efficiency is only 45.4% for P_{N2} at 45.6 kPa. The non-monotonous variation trend implies that factors which enhance and weaken the heat transfer work simultaneously with the increasing initial environmental partial pressure. The mechanism analysis will be conducted based on three key aspects including flash evaporation, convection and boiling. The flash evaporation rate is proportional to the difference between the saturated pressure and the equilibrium pressure [23]. It means that higher environmental partial pressure lowers the flash evaporation rate, which is not conducive to the heat transfer. Nevertheless, lower flash evaporation rate allows more fine droplets to reach the surface, which enhances the heat transfer. Meanwhile, higher environmental partial pressure decreases the coolant latent heat as shown in Figure 7[1)], which is also adverse to the heat transfer. In addition, higher environmental partial pressure slows down the droplet velocity and damps the impact effect on the evaporator surface, which is not beneficial for the convection.

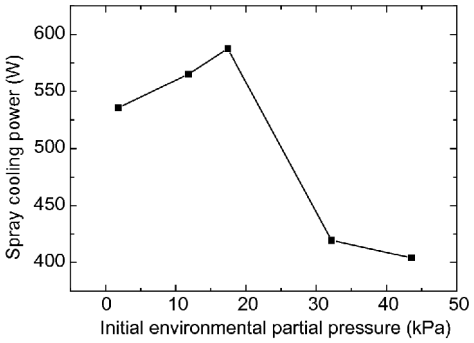

Figure 5 Variation of the spray cooling power with the initial environmental partial pressure for P_{R21}=28.0 kPa.

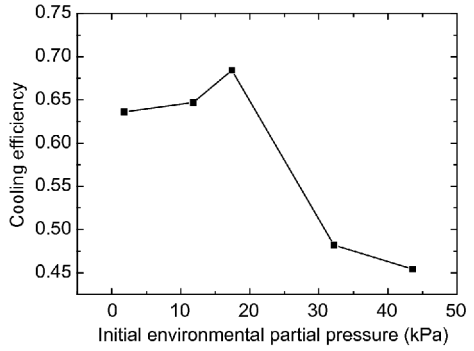

Figure 6 Variation of the cooling efficiency with the initial environmental partial pressure for P_{R21}=28.0 kPa.

1) National Institute of Standards and Technology. Thermophysical Properties of Fluid Systems. https://webbook.nist.gov/chemistry/fluid/

Besides the mechanisms for flash evaporation and convection mentioned above, the boiling heat transfer of the liquid R21 on the evaporator surface will also follow the boiling heat transfer curve, as shown in Figure 8 [24]. Actually, it is the superheat that is directly affected by the total pressure. The relationship between the average superheat and the total pressure is shown in Figure 9. It is noticed that as the total pressure increases the average superheat decreases. Correspondingly, the heat flux will go along with the boiling heat transfer curve from transition boiling to nucleate boiling, which leads to a variation trend that the spray cooling power first increases to a maximum and then decreases.

Experiments for P_{R21}=38.9 kPa and the temperature of water at the inlet of the evaporator at 26.1°C are conducted. The initial environmental partial pressure ranges from 1.47 kPa to 44.0 kPa. The variation of spray cooling power and cooling efficiency are plotted with the total pressure in Figures 10 and 11 respectively. It can be found that no optimal total pressure shows up and the spray cooling power and cooling efficiency decrease monotonically with the total pressure increasing. The reason is that the heat transfer is in the nucleate boiling regime in the entire experimental range

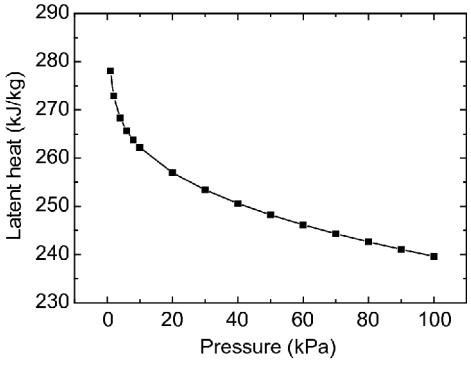

Figure 7 Latent heat of R21 varying with pressure[1)].

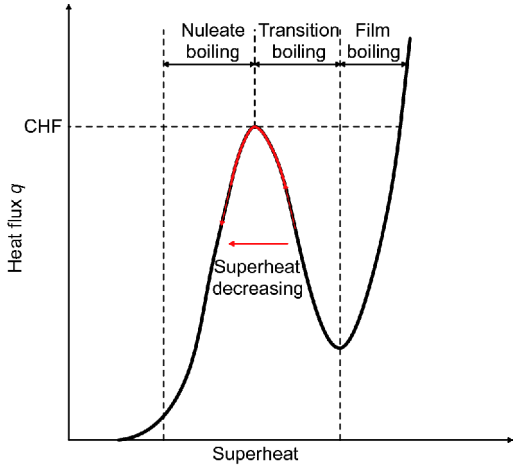

Figure 8 (Color online) Schematic of the boiling heat transfer curve based on ref. [24].

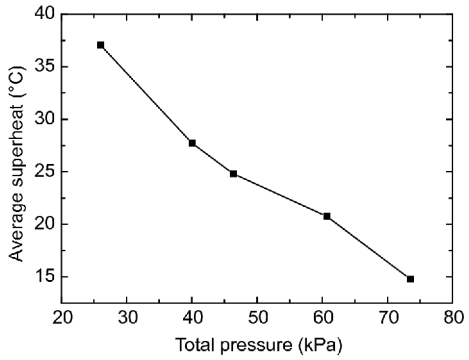

Figure 9 Variation of the average superheat with the total pressure for P_{R21}=28.0 kPa.

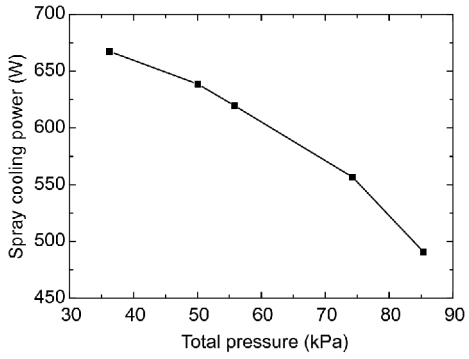

Figure 10 Variation of the spray cooling power with the total pressure for P_{R21}=38.9 kPa.

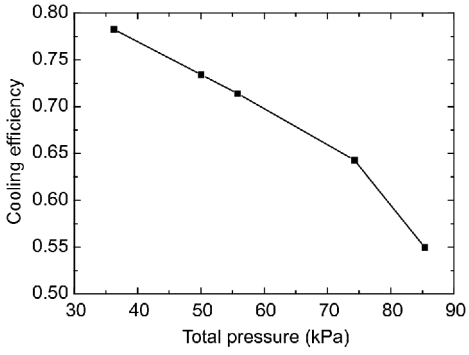

Figure 11 Variation of the cooling efficiency with the total pressure for P_{R21}=38.9 kPa.

and the heat flux decreases along the boiling heat transfer curve with the decrease in superheat.

Experiments by maintaining the initial environmental partial pressure at constant and varying the vapor partial pressure are also performed. The vapor partial pressure is adjusted by changing the inlet temperature of the condensing heat exchanger in the condensing chamber. The initial environmental partial pressure is kept at 1.8 kPa, while the vapor partial pressure ranges from 23.1 kPa to 64.5 kPa. Figures 12 and 13 show the variation of spray cooling power and cooling efficiency with the vapor partial pressure re-

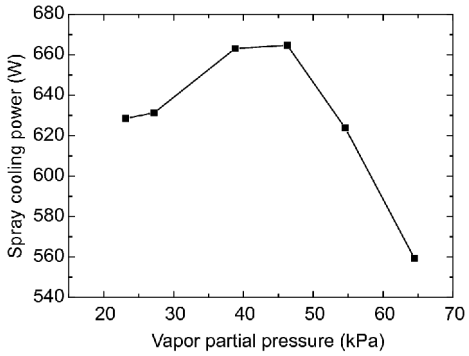

Figure 12 Variation of the spray cooling power with the vapor partial pressure.

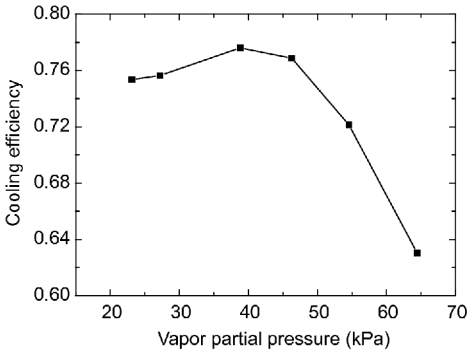

Figure 13 Variation of the cooling efficiency with the vapor partial pressure.

spectively. The spray cooling power increases from 628.5 W to 664.7 W at first, and then drops to 548.0 W. The cooling efficiency behaves in the same way, increasing from 75.4% to 77.6% at first, and then reducing to 63.0%. All in all, it can be concluded that decreasing the initial environmental partial pressure or the vapor partial pressure cannot always benefit the heat transfer.

4 Conclusions

The flash spray cooling system is established to investigate the spray cooling performance under reduced pressures. Nitrogen is used to create different initial environment partial pressures and a refrigerator system is used to maintain or adjust the vapor partial pressure. The influences of spray flow rate and different pressures on spray cooling power and cooling efficiency are investigated. The results show that the spray cooling power increases monotonically with the increasing spray flow rate, while the cooling efficiency decreases with the increasing spray flow rate. The reason for the decreasing cooling efficiency is that larger spray flow rate causes more loss of R21 droplets. Decreasing the initial environmental partial pressure or the vapor partial pressure cannot always enhance the heat transfer. There is an optimal value to optimize the heat transfer for the initial environmental partial pressure or the vapor partial pressure. The mechanisms are addressed in three key aspects including flash evaporation, convection and boiling. Higher environmental partial pressure lowers the flash evaporation rate, decreases the latent heat of R21 and damps the droplet impact effect, which are not conducive to the flash evaporation and the convection. However, lower flash evaporation rate allows more fine droplets to reach the surface, which is beneficial to the heat transfer. In addition, the heat transfer will go along with the boiling heat transfer curve from transition boiling to nucleate boiling with the decreasing average superheat, as a result, the spray cooling power first increases to a maximum and then decreases.

This work was supported by the National Natural Science Foundation of China (Grant No. 51376101), and the National Science Fund for Creative Research Groups (Grant No. 51621062).

1 Kang B S, Choi K J. Cooling of a heated surface with an impinging water spray. KSME Int J, 1998, 12: 734–740
2 Zhou Z, Chen B, Wang R, et al. Coupling effect of hypobaric pressure and spray distance on heat transfer dynamics of R134a pulsed flashing spray cooling. Exp Thermal Fluid Sci, 2016, 70: 96–104
3 Wang Y, Liu M, Liu D, et al. Experimental study on the effects of spray inclination on water spray cooling performance in non-boiling regime. Exp Thermal Fluid Sci, 2010, 34: 933–942
4 Xie N N, Hu X G, Tang D W. Experimental investigation on spray cooling in rectangular capillary micro-grooves. J Eng Therm, 2010, 31: 805–809
5 Silk E A, Kim J, Kiger K. Spray cooling of enhanced surfaces: Impact of structured surface geometry and spray axis inclination. Int J Heat Mass Transfer, 2006, 49: 4910–4920
6 Silk E A, Kim J, Kiger K. Impact of cubic pin finned surface structure geometry upon spray cooling heat transfer. In: Proceedings of the Asme International Electronic Packaging And Technical Conference. San Francisco, 2005
7 Zhang Z, Jiang P X, Ouyang X L, et al. Experimental investigation of spray cooling on smooth and micro-structured surfaces. Int J Heat Mass Transfer, 2014, 76: 366–375
8 Rybicki J R, Mudawar I. Single-phase and two-phase cooling characteristics of upward-facing and downward-facing sprays. Int J Heat Mass Transfer, 2006, 49: 5–16
9 Chen R H, Chow L C, Navedo J E. Effects of spray characteristics on critical heat flux in subcooled water spray cooling. Int J Heat Mass Transfer, 2002, 45: 4033–4043
10 Chen R H, Chow L C, Navedo J E. Optimal spray characteristics in water spray cooling. Int J Heat Mass Transfer, 2004, 47: 5095–5099
11 Sehmbey M S, Chow L C, Hahn O J, et al. Effect of spray characteristics on spray cooling with liquid nitrogen. J Thermophysics Heat Transfer, 1995, 9: 757–765
12 Cader T, Westra L J, Eden R C. Spray cooling thermal management for increased device reliability. IEEE Trans Device Mater Relib, 2004, 4: 605–613
13 Bostanci H, Van Ee D, Saarloos B A, et al. Spray cooling of power electronics using high temperature coolant and enhanced surface. In: Proceedings of the Vehicle Power and Propulsion Conference. Dearborn, 2009
14 Kim J. Spray cooling heat transfer: The state of the art. Int J Heat Fluid Flow, 2007, 28: 753–767
15 Han F Y. Study on Heat Transfer Performance, Enhancement, and Surface Temperature Non-Uniformity in Spray Cooling. Dissertation

for Dcotoral Degree. Heifei: University of Science and Technology of China, 2011
16 Jiang S, Dhir V K. Spray cooling in a closed system with different fractions of non-condensibles in the environment. Int J Heat Mass Transfer, 2004, 47: 5391–5406
17 Lin L, Ponnappan R. Heat transfer characteristics of spray cooling in a closed loop. Int J Heat Mass Transfer, 2003, 46: 3737–3746
18 Horacek B, Kiger K T, Kim J. Single nozzle spray cooling heat transfer mechanisms. Int J Heat Mass Transfer, 2005, 48: 1425–1438
19 Mudawar I, Bharathan D, Kelly K, et al. Two-phase spray cooling of hybrid vehicle electronics. IEEE Trans Comp Packag Technol, 2009, 32: 501–512
20 Timothy A B, Jordan L M, Asuncion C, Shuttle orbiter active thermal control subsystem design and flight experience. SAE Technical Paper, 1991
21 Golliher E, Romanin J, Kacher H,et al. Development of the compact flash evaporator system for exploration. SAE Technical Paper, 2007
22 Estes K A, Mudawar I. Correlation of sauter mean diameter and critical heat flux for spray cooling of small surfaces. Int J Heat Mass Transfer, 1995, 38: 2985–2996
23 Saury D, Harmand S, Siroux M. Experimental study of flash evaporation of a water film. Int J Heat Mass Transfer, 2002, 45: 3447–3457
24 Incropera F P, DeWitt D P, Bergman T L, et al. Fundamentals of Heat and Mass Transfer. New York: John Wiley & Sons, 2006